Vol 14 No 7, July 2005
1009-1963/2005/14(07)/1433-06

Chinese Physics

© 2005 Chin. Phys. Soc.
and IOP Publishing Ltd

High power red laser at 671nm by intracavity frequency doubling of a Nd:YVO_4 laser*

Yao Ai-Yun(姚爱云)[a], Hou Wei(侯 玮)[a], Li Hui-Qing (李惠清)[a], Bi Yong(毕 勇)[b], Li Rui-Ning(李瑞宁)[a], Geng Ai-Cong(耿爱丛)[a], Kong Yu-Peng(孔宇鹏), Cui Da-Fu(崔大复)[a], and Xu Zu-Yan(许祖彦)[a]†

[a] *Beijing National Laboratory for Condensed Matter Physics, Institute of Physics, Beijing* 100080, *China*

[b] *Academy of Opto-electronics, Chinese Academy of Sciences, Beijing* 100080, *China*

(Received 21 October 2004; revised manuscript received 25 February 2005)

This paper reports a high-power quasi-continuous wave (quasi-CW) source of red laser at 671nm obtained by intracavity frequency doubling of a double-end-pumped 1342nm Nd:YVO_4 laser, based on the nonlinear crystal LiB_3O_5(LBO) The average output power of 2.9W at 671nm was obtained at the incident pump power of 19.5W. The overall optical to optical efficiency is 14.9%. We have analyzed the influence of the optimal pump size, the optimal focal position and the reduction of the thermal effect on high output. The combination of double-end-pumping and the quasi-CW performance greatly reduces the thermal effect.

Keywords: quasi-continuous wave, double-end-pumped, thermal focal length
PACC: 6180B, 4260D, 4490

1. Introduction

Diode-end-pumped solid-state lasers have been attracting great interest due to their many good properties, for example, excellent beam quality, high efficiency, high reliability, compact size, and low root mean sequence (rms) noise, all of which make these lasers become increasingly more useful in industry, medical treatment and other domains; and other lasers such as flashlamp-pumped solid-state lasers and gas lasers can be replaced by them.[1] But the progress in scaling power is often impeded by the formation of an aberrated thermal lens within the active medium. The beam quality and the efficiency are also needed to be further improved. End-pumping solid-state lasers with side-cooling can provide much higher TEM_{00} efficiencies (>50%),[2,3] indicating that end-pumping is one of the most effective ways to match the sizes of the pump beam and the cavity mode. In addition, the maximum incident pump power is limited by thermal fracture of the laser crystal. Therefore, it is of primary importance to avoid thermally induced fracture, control thermal effect and optimize the overlapping efficiency.

In this paper, we report a quasi-continuous wave (quasi-CW) red laser at 671nm by intracavity frequency doubling of a double-end-pumped 1342nm Nd:YVO_4 laser, based on the nonlinear crystal LiB_3O_5 (LBO) The average output power of 2.9W at 671nm can be obtained at the incident pump power of 19.5W. The overall optical to optical efficiency is 14.5%. When designing this resonator, we first confirm the range of the fracture-limited pump power, guarantee the condition that the laser crystal does not crack, and then consider the optimization of the mode-to-pump beam ratio and the optimal overlapping efficiency. The influence of the pumping way and the pumping performance on the thermal effect is also discussed.

2. Theoretical analysis

Based on the space-dependent rate equation analysis, the output power $P_{\rm out}$ can be related to the input

*Project supported by the Innovation Program of the Chinese Academy of Sciences (Grant No KJCX1-05), the National High Technology Development Program of China (Grant No 2002AA311120), and the Council for Science and Technology of Beijing (Grant No H020420060060110).

†E-mail: zyxu@aphy.iphy.ac.cn

power $P_{\rm in}$ by[4]

$$P_{\rm out} = S_{\rm e} \times (P_{\rm in} - P_{\rm th}). \quad (1)$$

Both the pump threshold power P_{th} and the slope efficiency $S_{\rm e}$ depend on the match function F:

$$F(C/n, \alpha, L, \omega_{\rm l0}, \omega_{\rm p0}, z_0) = \frac{1}{1-\exp(-\alpha L)} \times \int_0^L \frac{\alpha\omega_{\rm l0}^2 \exp(-\alpha z)}{\omega_{\rm l0}^2 + [\omega_{\rm p0} + (C/n\omega_{\rm p0})\,|z - z_0|]^2}{\rm d}z, \quad (2)$$

which describes the spatial overlap of the pump beam and the cavity mode.[4] Here n is the refractive index of the active medium, C a constant that is characteristic of the beam quality, α the absorption coefficient of the laser crystal, L the crystal length; $\omega_{\rm l0}$ and $\omega_{\rm p0}$ are the beam waists of the cavity mode and the pump light, respectively. z_0 is the focusing position of the pump beam. The point z= 0 is taken to be at the pump surface of the active medium.

The overlapping efficiency η_0 can be written as

$$\eta_0 = \frac{F(C/n, \alpha, L, \omega_{\rm l0}, \omega_{\rm p0}, z_0)}{F(C/n, \alpha, L, \omega_{\rm l0}/\sqrt{2}, \omega_{\rm p0}, z_0)}. \quad (3)$$

The range of F is from 0 to 1, i.e. the lowest threshold and the highest slope efficiency that can be achieved at the maximum value of the match function. For $L \gg 1/\alpha$,[5] by considering no condition on the length of the active medium, Eq.(2) can be simplified as

$$F(\beta, \omega_{\rm l0}, \omega_{\rm p0}, \xi_0, d) = \frac{1}{1-\exp(-d)} \times \int_0^d \frac{\omega_{\rm l0}^2 \exp(-\xi)}{\omega_{\rm l0}^2 + [\omega_{\rm p0} + (\beta/\omega_{\rm p0})\,|\xi - \xi_0|]^2}{\rm d}\xi, \quad (4)$$

by changing variable $d = \alpha L$, $\xi_0 = \alpha z_0$ and $\beta = C/n\alpha$.

In Eq.(4), the match function depends on the β and d, while the latter two depend on the pump beam quality and the properties of the active medium.

For a fibre-coupled laser diode, the value C can be calculated from the following equation:

$$\theta_{\rm p0} = \frac{C}{n\omega_{\rm p0}}. \quad (5)$$

The average pump size for a fiber-coupled laser diode can be written as

$$\varpi_{\rm p}(\beta, \omega_{\rm p0}, \xi_0, d) = \frac{\int_0^L (\omega_{\rm p0} + (C/n\omega_{\rm p0})\,|z - z_0|)\exp(-\alpha z){\rm d}z}{\int_0^L \exp(-\alpha z){\rm d}z} = \frac{\int_0^d (\omega_{\rm p0} + (\beta/\omega_{\rm p0})\,|\xi - \xi_0|)\exp(-\xi){\rm d}\xi}{\int_0^\infty \exp(-\xi){\rm d}\xi}. \quad (6)$$

After some algebraically manipulating and differentiating with respect to ξ_0 and $\omega_{\rm p0}$,

$$\frac{\partial \varpi_{\rm p}(\beta, \omega_{\rm p0}, \xi_0, d)}{\partial \xi_0} = 0, \quad (7)$$

$$\frac{\partial \varpi_{\rm p}(\beta, \omega_{\rm p0}, \xi_0, d)}{\partial w_{\rm p0}} = 0, \quad (8)$$

the optimum focal position $z_{0,\rm opt}$and the optimum value of $\omega_{\rm p0}$ at a fixed β can be obtained:

$$z_{0,\rm opt} = \frac{1}{\alpha} \ln\left(\frac{2}{1+\exp(-d)}\right), \quad (9)$$

$$\omega_{\rm p0,opt} = \left\{\beta\left[\left(\ln\left(\frac{2}{1+\exp(-d)}\right) - 1\right)\coth\left(\frac{d}{2}\right) + \frac{1+\exp(-d) - d\exp(-d)}{1-\exp(-d)}\right]\right\}^{\frac{1}{2}}. \quad (10)$$

Figure 1 is the calculated curve for the optimum focal position $z_{0,\rm opt}$ versus the active medium length. It can be seen that the optimum focal position is about 0.8mm from the laser crystal end face. Figure 2(a) shows the variation of the optimum values of $\omega_{\rm p0}$ versus the active medium length. Figure 2(b) is the calculated curve of the optimum value of $\omega_{\rm p0}$ against the beam quality. The optimum value of $\omega_{\rm p0}$ is 0.35–0.4mm. Also experiment is carried out to find the optimum focal position $z_{0,\rm opt}$ and the optimum value of $\omega_{\rm p0}$. Figures 3 and 4 are the experimental results. Figure 3 shows the optimal focal position is about 0.8mm from the laser crystal end surface. Figure 4 shows that when the pump-to-mode ratio $\omega_{\rm p0}/\omega_0$ is 0.75, meaning the $\omega_{\rm p0}$ is in the range of 0.35–0.4mm when the pump beam radius ω_0 is 400mm, the output can achieve the maximum.

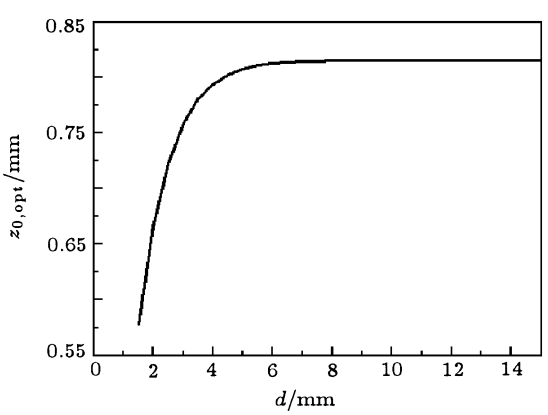


Fig.1. The optimum focal position $z_{0,\rm opt}$ as a function of active medium length.

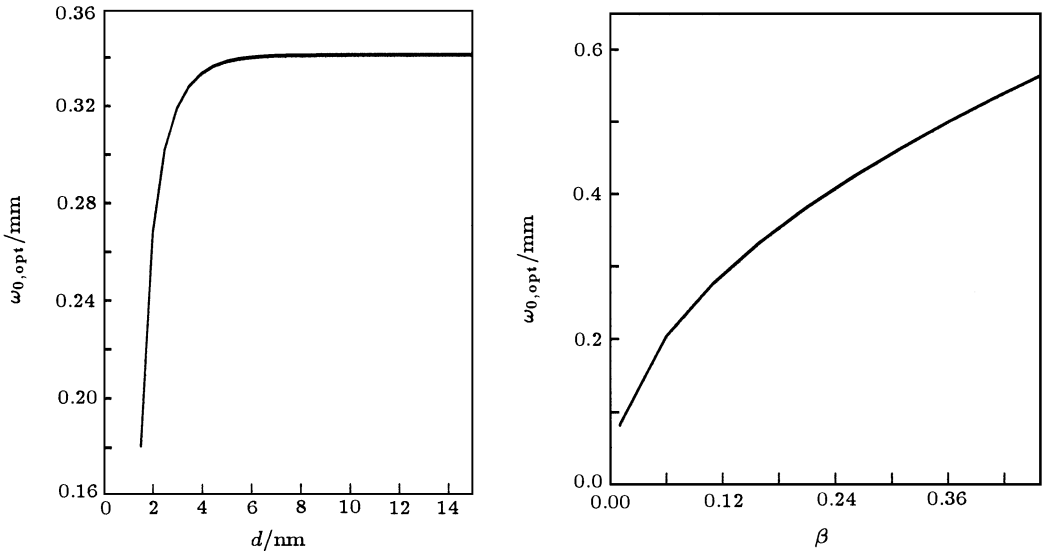


Fig.2. (a) The optimum focal position $\omega_{0,\mathrm{opt}}$ as a function of active medium length. (b) The optimum focal position $\omega_{0,\mathrm{opt}}$ as a function of the beam quality.

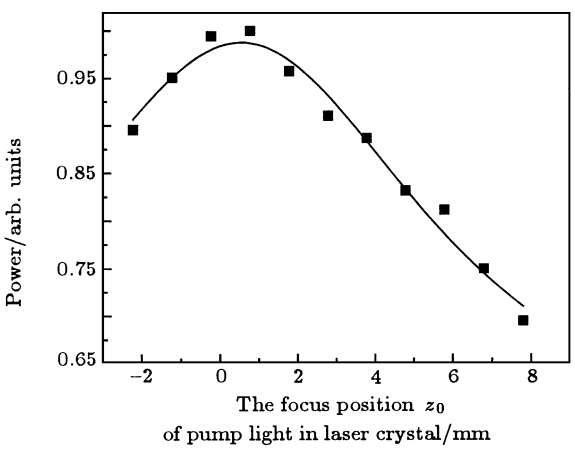


Fig.3. The experimental result of the optimum focal position z_0.

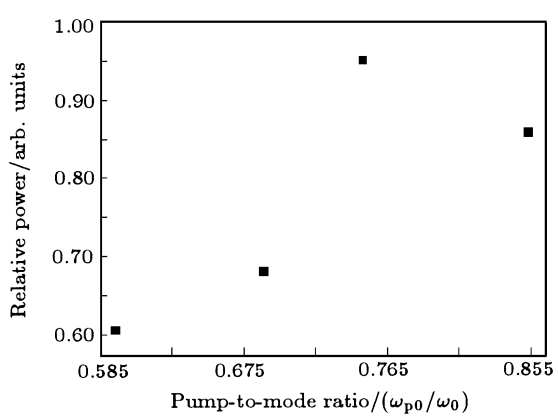


Fig.4. The experimental result of the optimum value of ω_{p0}.

3. Experiment

3.1. Experimental setup

Figure 5 is the experimental setup, in which the laser crystal is double-end-pumped or single-end-pumped by a fibre-coupled diode array through a focusing system. The LD can be operated in CW or quasi-CW operation mode. For the quasi-CW operation, its pulse width and repetition are 2ms and 500Hz, respectively, with a duty cycle of 1:1. The beam from the LD is coupled into the resonator by the focusing system. The LD is made from 30W fibre-coupled diode laser arrays (coherent corporation) with the central output wavelength of the lasers being 808nm at 25°C. The fibres are combined into a round bundle of 0.8mm diameter with a numerical aperture of 0.22. The pump beam is collimated and focused on the crystal by a pair of plane/convex lenses. The resonator consists of four mirrors. Both mirrors M1 and M2 are flat, being coated for antireflection at 808nm and 1064nm (T >93.5%) and for high reflection at 1342nm (R >99.8%). Mirror M3, with a convex radius of 100mm, is coated for high-reflection at both 1342nm and 671nm. Mirror M4, with the same convex radius as that of M3, is coated for high-reflection at 1342nm and antireflection at 671nm. The special coatings will guarantee the suppression of lasing at the strong transition of 1064nm. The laser crystal is Nd:YVO_4 with nominal Nd-ion doping of 0.3% and dimensions of $3 \times 3 \times 15\mathrm{mm}^3$, provided by Fujian Castech Crystals. Both end surfaces of the crystal are coated for antireflection at 808nm and at 1342nm. The z-cut LBO crystal has dimensions of $3 \times 3 \times 20\mathrm{mm}^3$ with an orientation for type II noncritical phase match

(NCPM) second harmonic generation (SHG). For frequency doubling at 1342nm, NCPM in type II LBO occurs at 39.5°C, which is slightly higher than room temperature and so could be easily controlled. In our experiment we maintain the phase matching temperature by heating the LBO crystal in an oven, with a controlled temperature accuracy of 0.1°C. The laser crystal is wrapped in a thin indium foil and kept in a small copper holder which is fixed in a copper housing cooled by distilled water at a temperature of 25°C.

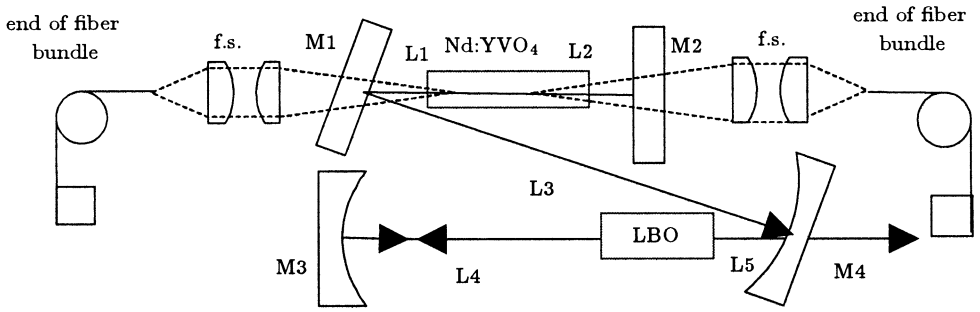


Fig.5. Double-end-pumped experimental setup with a folded four - mirror resonator. L1 and L2 denote the distances between M1 and the laser crystal, M2 and the crystal, respectively. L3 and L4 denote the distances between M1 and M4, M3 and M4, respectively. L5 is the distance between LBO and Mirror M4, and f.s. denotes the focusing system.

3.2. Result analysis

The laser performance is investigated in both CW and quasi – CW operation modes. Figure 6 shows the experimental result. To our knowledge, this is the highest quasi-CW output at 671nm from SHG of a double-end-pumped Nd:YVO_4 laser. The maximum average power is 2.9W for quasi – CW and 1.6W for CW operation at pump power of 19.5W and 20W, respectively. As can be seen in Fig.6, the quasi-CW intracavity SHG efficiency is 14.9%, and CW intracavity SHG efficiency is 8.0%. Obviously, the output power and the efficiency in the quasi – CW mode is higher than that in the CW mode. The solid curves show the corresponding theoretical calculations based on the Smith model with a simple plane-wave model, in which, the beam distribution inside the resonator is independent of that of the pump power and hence there is no thermal effect. The second-harmonic power is calculated using the following equation:[6,7]

$$P_{2\omega} = \frac{\pi w^2}{8k} I_s^2 \left\{ -\left(k + \frac{L}{I_s}\right) + \left[\left(k + \frac{L}{I_s}\right)^2 + 4\frac{k}{I_s}\left(2K_c P_i - L\right)\right]^{\frac{1}{2}} \right\}^2, \quad (11)$$

$$k = \frac{4\pi^2}{\lambda_\omega^2} z_0 \frac{d_{\text{eff}}^2 l^2}{n^3} \frac{w^2}{w_s^2} \beta, \quad (12)$$

where w_s and w are the beam sizes in LBO crystal and Nd:YVO_4 crystal, respectively; P_i is the incident LD pump power; K_c is the pump coupling coefficient, L is the resonator loss, z_0= 377Ω is the vacuum impedance. I_s is the saturation intensity ($I_s = \frac{h\nu}{\tau\sigma_f}$, where, τ=110μs and σ_f=6.0× 10^{-19}cm^2) at 1342 nm transition in Nd:YVO_4,[8] l is the length of LBO. The factor $2 < \beta \leq 4$ takes into account the phase match between the fundamental and the second harmonics in the second pass. In Eq.(2), l=20mm, d_{eff}=0.65pm/V, n=1.6, ω=700μm and ω_s=90μm. The intracavity loss and the pump coupling coefficient are determined, by the Findlay–Clay analysis,[9] to be L=0.05 and K_c=0.02W^{-1} in our experiment. Comparing the experimental results with the theoretical calculation, we noted that there is a little difference between them, which may be attributed to using the simple plane-wave model and assuming no depleted 1342nm pump wave for the theoretical calculation.

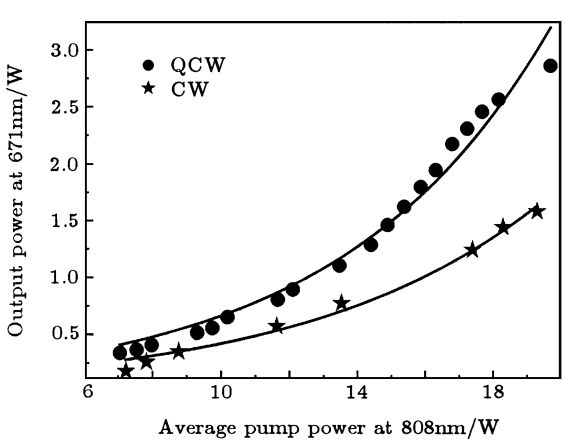


Fig.6. Comparison of the CW operation and quasi-CW operation. Dots: quasi-CW operation; Stars: CW operation.

We have also calculated the thermal distribution difference between the single-end-pumping and double-end-pumping ways using finite element analysis. Figures 7(a) and 7(b) are the results when the laser crystal absorbs the same amount of heat in single-end-pumping and double-end-pumping operation. The heat is mainly distributed at the two end surfaces of the laser crystal when operation double-end-pumping. But by single-end-pumping, the heat is mainly distributed in one end surface of the laser crystal. The maximum temperature differences between the border and the centre in the end surface are 7.6°C and 15.2°C, respectively, which means that the temperature gradient is smaller in the former case, and the heat absorbed by the laser crystal distributes more uniformly. This makes the temperature gradient and index of refraction more uniform. Thus for the same amount of heat absorbed by the laser crystal, the thermal focal length is longer and we can pump more power into the crystal and enhance the fundamental output.

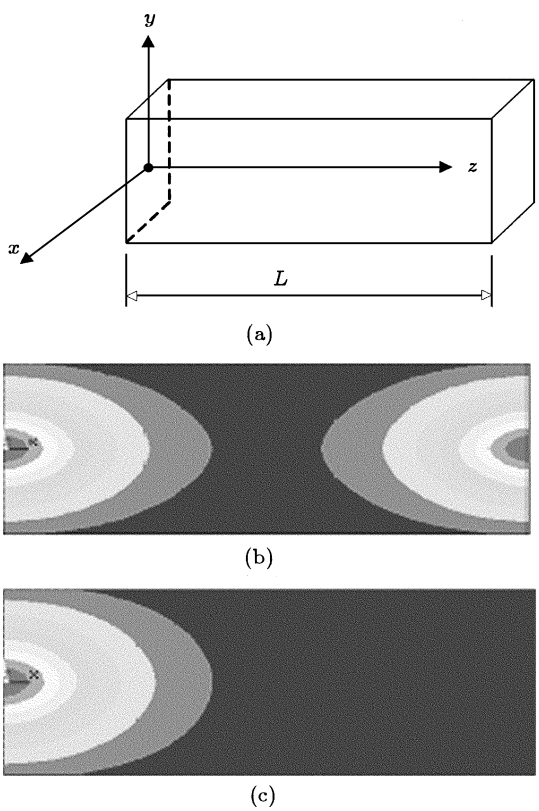


Fig.7. (a) The geometry of the laser crystal. (b), (c) The calculated thermal distribution at the longitudinal cross section of laser crystal: (b) with two lenses inside (c) with one lens inside. Vertical axis represents the temperature distribution along y direction; horizontal axis the distribution along the laser propagation z direction in the laser crystal.

The quasi-CW performance of the pump beam also influences the thermal effect. If the laser crystal absorbs the same amount of average pump power, the temperature in the laser crystal in CW operation is higher than that in quasi-CW operation. In quasi-CW laser operation, the heat in laser crystal is transferred faster, which makes the thermal focal length longer, the divergence angle smaller, then the mode volume larger; and thus enhances the output power. The thermal focal lengths were measured by means of resonator transform circle approach,[10−12] which are shown in Fig.8 for both CW and quasi-CW operations. It shows that when the laser crystal absorbed the same amount of heat pumped by CW and quasi-CW operations, the thermal focal length produced by the latter will be longer than that produced by the former. The thermal focal length is about 203.3mm for CW operation and 244.7mm for quasi-CW operation at the same pump power of 19.5W. Thus the combination of double-end-pumping with the quasi-CW performance pump power greatly reduces the thermal effect.

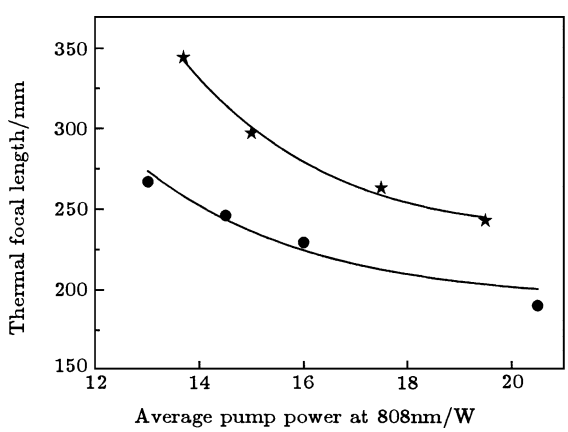


Fig.8. The measured thermal focal lengths versus the incident pump power in CW operation and in quasi-CW operation. Stars: in quasi-CW operation; dots: in CW operation; solid curves are the fitted results.

4. Summary

In summary, we have presented a compact, high power 671nm quasi-CW red source based on an intracavity frequency doubling of double-end-pumped Nd:YVO_4 laser. The average output power of 2.9W at 671nm is obtained at the incident pump power of 19.5W with the overall optical to optical efficiency is 14.9%. The optimal focus position and the optimal radius of oscillating mode contribute to the match between the pump beam and the oscillating mode. The

combination of double-end-pumping and the quasi-CW performance of the pump beam greatly reduce the thermal effect.

References

[1] Inoue Y, Konno S, Kojima T and Fujikawa S 1999 *IEEE J. Quantum Electron.* **35** 1737

[2] Chen Y F, Huang T M, Wang C L and Lee L J 1998 *Appl. Optics* **37** 5727

[3] Hodgson *et al* 1999 *Proc. SPIE* **3611** 119

[4] Chen Y F, Kao C F and Wang S C 1997 *Opt. Commum.* **133** 517

[5] Chen Y F and Kuo H J 1998 *Opt. Lett.* **23** 846

[6] Agnesi A, Guandalini A and Reali G 2002 *J. Opt. Soc. Am.* B **19** 1078

[7] Smith R G 1970 *IEEE J. Quantum Electron.* **6** 215

[8] Tucker A W, Birnbaum M, Fincher C L and Elder J W 1977 *J. Appl. Phys.* **48** 4907

[9] Findly D and Clay R A 1966 *Phys. Lett.* **20** 277

[10] Song F *et al* 2002 *Appl. Phys. Lett.* **81** 2145

[11] Laures P 1967 *Appl. Opt.* **6** 747

[12] Koechner W 1999 *Solid-State Laser Engineering* 5th Ed., (Berlin: Springer)